DETC2018-85696

POINT-BASED VIRTUAL ENVIRONMENT FOR SUPPORTING DETERIORATION DIAGNOSYS OF PRODUCTION FACILITIES

Yuki Shinozaki
The University of Elector-Communications
Chofu, Tokyo, Japan

Hiroshi Masuda
The University of Elector-Communications
Chofu, Tokyo, Japan

ABSTRACT

Maintenance of production facilities is important in various industries. Since production facilities degrade their original functions during their long life-cycle, it is necessary to periodically make deterioration diagnosis and renovate to restore functions. In recent years, the terrestrial laser scanner allows us to capture dense point-clouds from large production facilities. Point-based virtual environment is promising for supporting maintenance of production facilities. In this paper, we discuss the deterioration diagnosis of production facilities based on point-clouds when the original shapes of production facilities are unknown. As an example of production facilities, we consider the blast furnace, which is mainly used to produce metals from molten materials. We classify deterioration on the blast furnace as wearing, scaffolding, and cracks, and automatically detect them from point-clouds. In our method, the normal wall shape is estimated by fitting low-resolution B-spline surfaces to point-clouds, and deterioration is detected as the difference between the reference surface and the point-clouds. While wearing and scaffolding regions are relatively large, cracks are thin lines. In order to detect different scales of deterioration, we introduce the reference surfaces with multiple resolutions. In our experiments, the three types of deterioration could be successfully detected from dense point-clouds.

1. INTRODUCTION

Maintenance of production facilities is important in various industries, such as manufacturing, heavy industry, energy, materials, chemistry, and so on. Since production facilities degrade their original functions during their long life-cycle, it is necessary to periodically make deterioration diagnosis and renovate to restore functions.

In recent years, the terrestrial laser scanner has significantly improved and it has become possible to acquire dense point-clouds from large production facilities. Fig.1 shows an example of terrestrial laser scanner. The latest terrestrial laser scanner can acquire one million coordinates per second within 100 to 300 m.

Fig.1: Terrestrial laser scanner.
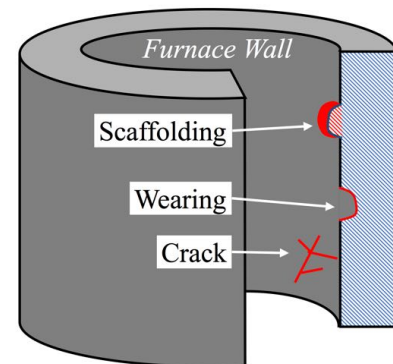
Fig. 2: Deterioration modes

Our research goal is to develop virtual environment for supporting maintenance of production facilities. Based on dense point-clouds of production facilities, we have developed a collision detection system to support renovation of production lines [Niwa], and a virtual reality system for supporting visual inspection of factories [Okamoto].

As a new application based on point-clouds, we consider a method for diagnosing deterioration caused by shape changes of production facilities. Depending on the type of production

facility, there are various degradation modes, such as deformation, wearing, crack, and scaffolds. Such shape changes can be detected if the old point-cloud and the current point-cloud are acquired at different times and their differences are investigated. However, it is difficult to apply this technique to actual production facilities, because the repair cycles of production facilities are often very long, and point-clouds of old situations are rarely preserved. In addition, even if CAD models or drawings of production facilities are preserved, they are often different from the current shapes because of large construction tolerances and repeated renovation. In such cases, change detection techniques cannot be applied unless the normal shapes can be estimated by using available data.

In this paper, we discuss the deterioration diagnosis of production facilities based on point-clouds when the original shapes of production facilities are unknown. To estimate normal shapes, we suppose that the original shape of a production facility consists of a smooth surface and the deteriorated regions consist of irregular convex or concave shapes on the smooth surface.

As an example of production facilities, we consider the blast furnace, which is mainly used to produce metals from molten materials. The inside wall of the blast furnace is deteriorated after long term use. In conventional deterioration diagnosis, the inspector visually estimates the amount of deterioration and identifies a need for maintenance of the furnace. However, visual inspection highly depends on individual skills and experiences, and the inspector does not quantitatively investigate the degree of deterioration. To solve these problems, we introduce deterioration diagnosis based on point-clouds.

The main deterioration modes of the blast furnace are scaffolds, wearing and cracks on the inside wall surfaces, as shown in Fig. 2. Scaffolding and wearing regions have relatively large areas whereas cracks are very thin regions. The scaffold is a region where molten metal adheres. The wearing is caused when the wall is partly peeled. The crack is caused on the wall as thin lines and grows over time.

In order to perform deterioration diagnosis using point-clouds, it is necessary to detect scaffolds, wearing, and cracks by estimating the normal wall surface. In this paper, the normal wall surface is referred to as a reference surface. The reference surface typically consists of a combination of approximately cylinders and cones. However, the reference surface is not an exact rotating surface but a distorted surface because of large construction tolerances. It is necessary to consider slightly distorted cylinders and cones as the reference surface for detecting deterioration.

There are many studies for extracting primitive surfaces from point-clouds. Masuda, et al. [1, 2] and Kawashima, et al. [3] extracted cylinders and planes from point-clouds captured using terrestrial laser scanners and created 3D models of the pipe structure in engineering plants. Nan, et al. [4] and Tang, et al. [5] were extracted wall planes from the point-clouds. However, they extracted only ideal planes or cylinders, and did not discuss deteriorations.

Mizoguchi et al. [6] detected wearing regions of deteriorated bridge piers using point-clouds. They assumed that the shapes of normal bridge piers were precise planes, and they detected deterioration as the difference between estimated ideal plane and the measured points. In their method, the reference plane was calculated using healthy planar regions. However, their method cannot be applied to our case, because the healthy regions are not precise cylinders or cone in the case of a furnace wall.

Nespeca et al. [7] proposed a method for detecting degradations by dividing a distorted plane into several planar regions. They calculated reference planes by locally fitting planes. Their approach is effective when the object consists of planes. However, when the object consists of distorted cylinders or cones, it is difficult to stably fit cylinders and cones to local points.

In this research, we aim to detect wearing, scaffolding and cracks on the wall surface of a blast furnace using point-clouds. We captured point-clouds of a blast furnace from multiple positions. In our previous research, we developed a method for detecting relatively large wearing and scaffolding regions [8]. In this paper, we discuss methods to detect all of wearing, scaffolding, and crack regions. Since cracks are very thin lines, we introduce multiple reference surfaces with different resolutions. Then we detect deteriorations with different scales.

Fig.3: Point-cloud of a blast furnace

2. OVERVIEW

Fig. 3 shows the point-cloud of a blast furnace. The total number of points is about 466 million points. The laser scanner was FARO Focus 3D X130 [9]. In this paper, we explain our method using this example. This furnace consists of two cylindrical surfaces, a conic surface, and a torus fillet. The height is about 22 m, and the maximum perimeter is about 27 m.

This point-cloud consists of 12 point-clouds captured at different scanner positions. These point-clouds were transformed to the world coordinates system. In point processing, this transformation is called as registration. We registered point-clouds using a commercial software.

The outline of our method is shown in Fig. 4. First, each of point-clouds is converted to a wireframe model by connecting neighbor points. Then horizontal planes are generated at small intervals, and intersection points are calculated between the horizontal planes and the wireframe models. Since the furnace wall is approximately a rotating surface, the section shapes are nearly circles. Therefore, circles are extracted from intersection points on each horizontal plane. Then cylinders and cones are extracted by connecting section circles.

Using the center axis of cylinders and cones, coordinates of points are transformed into cylindrical coordinates. Since cylinders and cones are mapped to flat planes in the cylindrical coordinate system, measured points are also mapped close to planes. Then a B-spline surface is fitted to the transformed points and it is used as the reference surface.

If the B-spline surface has a lot of control points, it faithfully fits to the point-cloud. If it has only a small number of control points, it loosely fits to the point-cloud. Therefore, we use low-resolution reference surfaces for detecting relatively large wearing and scaffolding regions, and we use high-resolution ones for detecting thin cracks.

We introduce different methods for detection of wearing and scaffolding and detection of cracks. The sizes of cracks are often smaller than registration errors, which are caused when multiple point-clouds are merged in the world coordinate system. Therefore, cracks are detected from each point-cloud and then the detected cracks are transformed and merged.

Finally, we merge three types of deterioration, and visualize the overall deteriorations.

3. DETECTION OF WEARING AND SCAFFOLDING

3.1 Extraction of Cylinders and Cones

First, cylinders and cones are extracted from the point-cloud. Several researchers have proposed methods for extracting cylinders and cones from point-clouds. Lucacs, et al. [10] proposed a faithful least-squares fitting method to calculate the implicit function of a surface using nonlinear optimization. Masuda, et al. [11] extracted surfaces from noisy point-clouds using robust estimate. Schnabel, et al. [12] extracted surfaces from noisy point-clouds using the RANSAC method. However, since cylinders and cones of the blast furnace are considerably distorted, it is difficult to stably calculate implicit surfaces.
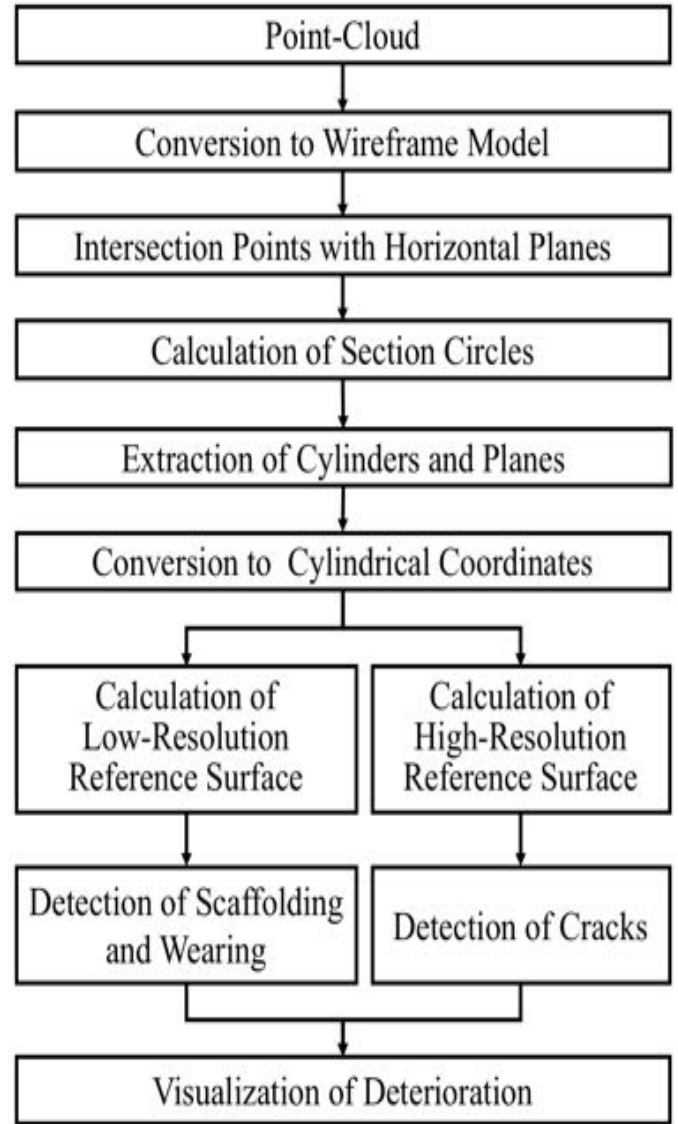
Fig.4: Outline of the method.

Therefore, we calculate section circles from point-clouds, because the section shapes of a rotational surface are circles.

We suppose that point-clouds are stored in the PTX format, in which 3D coordinates are represented using the scanner-centered coordinate system. Since the direction of the laser beam is rotated along azimuth angle θ and zenith angle φ, points can be mapped on the grid in (θ, φ) space, as shown in Fig. 5. We convert a point-cloud into a wireframe model by connecting adjacent points on this grid. Fig. 6(a) shows a wireframe model generated from a point-cloud.

Fig.5: Points in (θ, φ) space.
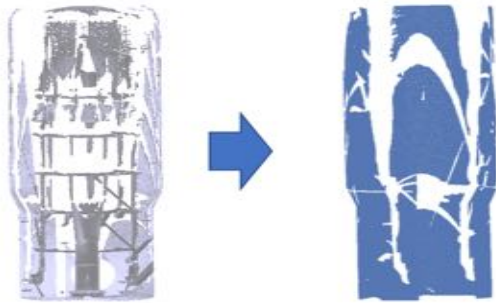
(a) Converting point-cloud to wireframe model
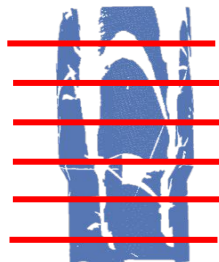
(b) Intersection with horizontal plane
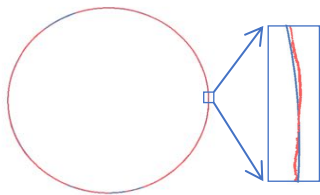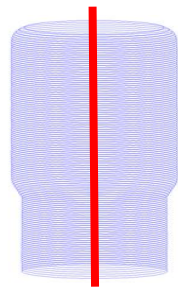
(c) Circle fitting　　　(d) Center line fitting

Fig.6: Extraction of section circles

Then the wireframe model is sliced using horizontal planes , as shown in Fig. 6(b), and the intersection points are calculated. This process is applied to all point-clouds, each of which was captured at a different scanner position. Then intersection points are merged on each section planes.

Since the cross-section curve of the furnace wall is approximately circular, a circle is detected on each section plane using the RANSAC method. Since the furnace walls are not an exact rotating surface, the threshold of the RANSAC method must be large. In this case, the threshold was set to10 cm. Fig. 6(c) shows an example of the detected circle. When circles are detected, the center line is detected by fitting a straight line to the centers of circles, as shown in Fig. 6(d).

When section circles and a center line are calculated, cylinders, cone, and torus are detected. We define the coordinate system so that the center line is the z axis, and we represent each circle as (r, z), where r is the radius. Then we map all section circles on the (r, z) plane.

We detect straight lines and circles from the mapped points. If a straight line perpendicular to the z axis is detected within a certain range, we regard the range as a cylindrical surface. If other straight lines are detected, we regard the range as a conic surface. If a circle is detected, we regard the range as a torus. Fig. 7(a) shows detected surfaces, and Fig. 7(b) shows the height of each surface.

3.2　Calculation of Reference Surface

In this paper, we analyze deteriorations on cylindrical surfaces and a conic surface. Deterioration is detected as the difference between the reference surfaces and the original measurement points, but the reference surface is unknown. Therefore, we estimate the normal surface and use it as the reference surface.

In our method, we use section points to estimate the reference planes. Since the number of total points is too large to store on RAM, we only maintain section points on RAM in our process. In this example, the section points were calculated at intervals of 5 cm and the total number of section points was 23.6 million.

Since the wall of the furnace seems to be originally distorted, we use bi-cubic B spline surface to represent the reference plane. The rotational surface is mapped to planar surfaces if it is represented in cylindrical coordinates. Therefore, we define the cylindrical coordinate system using the center axis, and represent (x, y, z) coordinates of section points to cylindrical coordinates (θ, ζ, r). Since all points are transformed near planes, planes are detected using the RANSAC method and the surface is divided into a set of planar regions, as shown in Fig.8.

We fit a uniform bi-cubic B-spline surface to each planar region. We represent a B-spline surface as $\mathbf{S}(u, v)$, section points as $\{\mathbf{P}_i\}$ $(i = 1,..,n)$, and control points of $\mathbf{S}(u, v)$ as $\{\mathbf{Q}_i\}$ $(i = 1,..,m)$. We suppose that each point $\mathbf{P}_i$ is represented as (θ_i, ζ_i, r_i). For fitting points to a B-spline surface, each point has to be parameterized as (u, v). We parameterize point $\mathbf{P}_i$ as (θ_i, ζ_i). Then we can obtain control points of a B-spline surface by solving the following minimization problem.

$$\underset{\{\mathbf{Q}_i\}}{\text{argmin}}\left\{\sum_{i=0}^{n}(\mathbf{S}(\theta_i,\zeta_i)-\mathbf{P}_i)^2 + \lambda \sum_{i=2}^{m-1}(\mathbf{Q}_{i-1}-2\mathbf{Q}_i+\mathbf{Q}_{i+1})\right\}$$

The second term of the function is introduced to avoid indefinite solutions when points are partially missing, as a hole in Fig. 8. The weight λ is specified as a small value. In this research, we specified $\lambda = 10^{-4}$.

3.3 Detection and Visualization of Deterioration

Deterioration is detected as differences between the reference surface and measured points. The resolution of the reference surface can be controlled using the number of control points. Since the original normal surface seems to be a smooth surface, we use a reference surface that loosely fit to points using a small number of control points.

To visualize differences between these reference planes and measured points, we generate difference maps. We visualize normal regions in green, wearing regions in blue, and scaffolding regions in red.
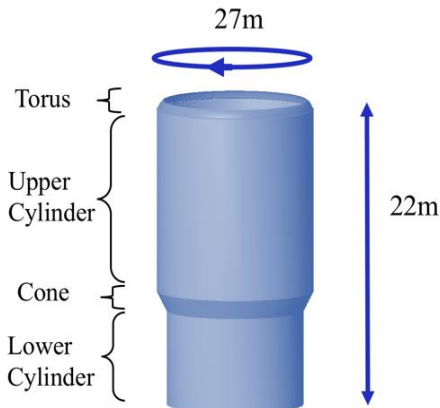
(a) Extracted surfaces

Torus	0.85 m
Upper Cylinder	13.75 m
Cone	1.10 m
Lower Cylinder	7.20 m

(b) Height of each surface

Fig.7: Detection of cylinders, a cone, and a torus
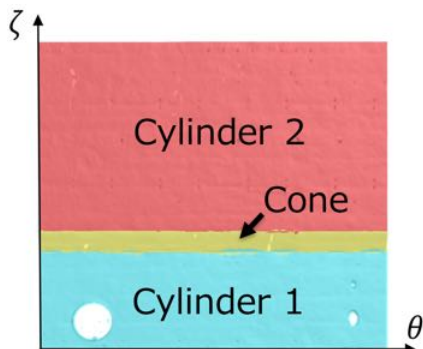
Fig.8: Points represented using cylindrical coordinates

Fig. 9 shows difference map when the reference surfaces with different resolutions are used. While deteriorations appear on loosely fitted reference surface, they disappear on tightly fitted one. Fig.10 shows scaffolding and wearing regions. In Fig. 11, deterioration is visualized as a height field with colors. In this figure, the deteriorations are exaggerated by increasing the heights five times. These results show that our method could detect scaffolding and wearing regions on the furnace wall.

(a) 8×8 segments   (b) 30×30 segments
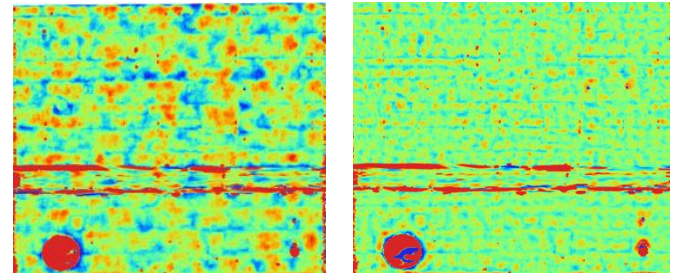
Fig. 9: Difference maps

(a) Scaffolding   (b) Wearing
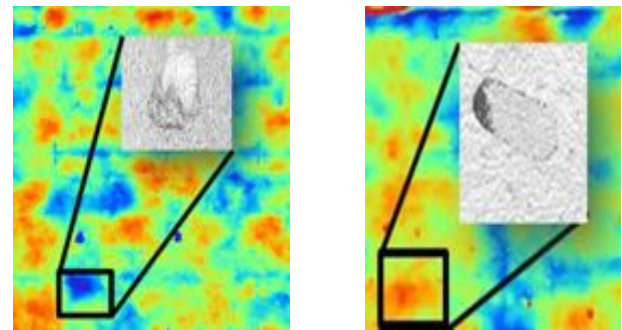
Fig.10: Detected deterioration
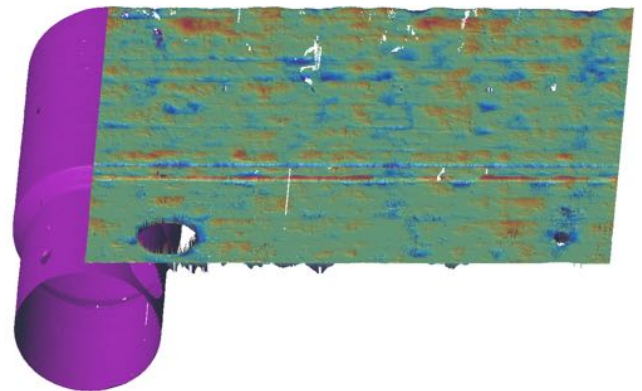
Fig.11: The height field with colors

4. DETECTION OF CRACKS

The method for wearing and scaffolding cannot detect small deteriorations such as cracks. Fig. 12 shows the difference map of cracks. Although cracks exist on the wall, they cannot be detected. Therefore, we consider another method for detecting cracks.

There are several reasons why crack detection fails. One reason is that point density is not enough to detect cracks. Therefore, in this paper, we consider only lower parts of points where the distances are relatively close to the scanner position.

However, cracks in Fig. 12 are close to the scanner position. Another reason is that small deteriorations are disappeared due to registration errors. Therefore, we detect cracks from individual point-cloud before point-clouds are registered and merged.

The third reason is that the resolution of the reference surface is too low to detect thin cracks. If the number of control points is increased and the reference surface tightly fits to wearing and scaffolding regions, only cracks can be detected as differences.

Fig. 13 shows deteriorations extracted from four point-clouds using the high-resolution reference surface. The number of control points of the B-spline surface was 30 x 30 in these cases. In all cases, small deteriorations can be detected by using the B - Spline surface with a larger number of control points as the reference surfaces.

However, it is not easy to visually recognize crack lines in Fig. 13. Since points are measured discretely by the laser scanner, deterioration points do not become continuous lines. Therefore, we convert them to lines by connecting neighbor points. In our method, when deteriorations are detected as discrete points, the Delaunay triangulation is applied to these points. If the distance between points in each triangle is smaller than a threshold, the points are connected as an edge. Fig. 14 shows connected points. As shown in this figure, cracks can be clearly visualized.

False cracks tend to be generated near the boundary of a point-cloud. This is because the laser scanner often produces outliers at the boundaries of objects. Therefore, we extract the boundary from each point-cloud and eliminate points detected as cracks near the boundary, as shown in Fig. 15.

In our method, cracks are detected from each point-cloud. Since there are missing points in each point-cloud because of occlusions, we subdivide the wall surface into rectangular cells, as shown in Fig. 16. Then we select point-clouds that cover each cell. If a point-cloud contains a sufficient number of points in a cell, cracks detected from the point-cloud is embedded in the cell.

In this example, we divided the wall surface with 100×100 cells. Fig. 17 shows the visualized result of cracks, in which cracks in each cell are unified.
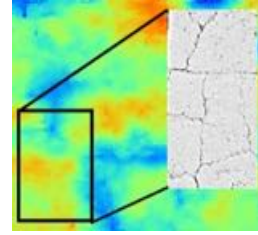
Fig.12: Failed to detect cracks

(a) Point-cloud 1　　　　(b) Point-cloud 2

(c) Point-cloud 3　　　　(d) Point-cloud 4
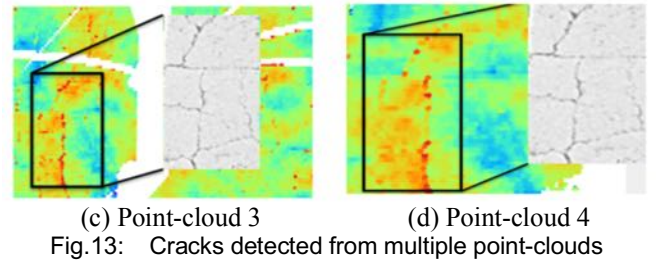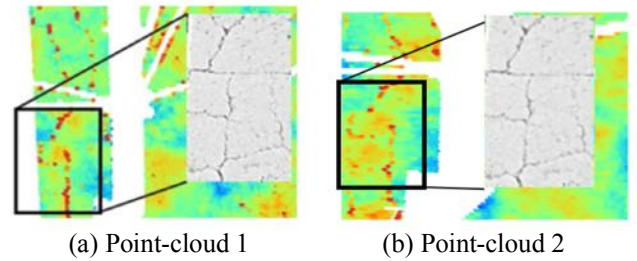
Fig.13:　Cracks detected from multiple point-clouds
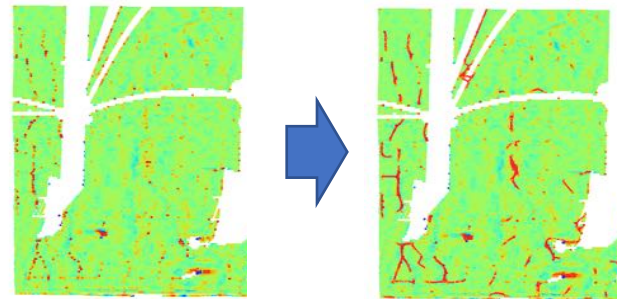
Fig.14: Lines of cracks
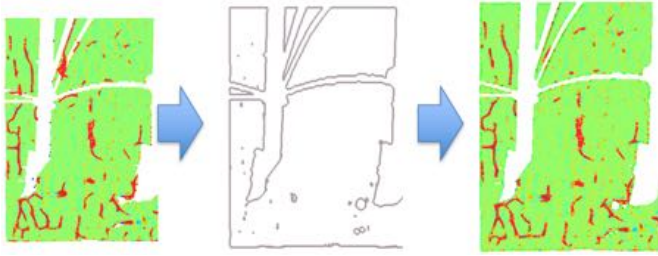
Fig.15:   Elimination of cracks near the boundary

Fig.16:   Cells generated by dividing the wall surface

Fig.17:   Merged cracks

Number of points	446 million points
Number of section points	23.6 million points

Tab. 1: Number of points

Wearing and Scaffolding Regions	3 min 32 sec
Cracks	18 min 45 sec

Tab. 2: CPU time for detecting deterioration
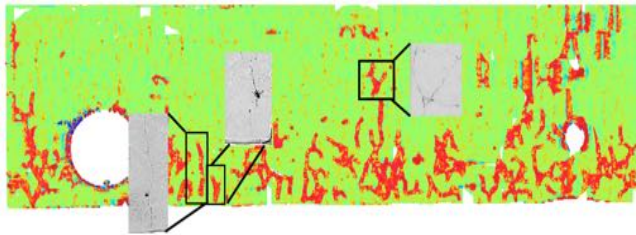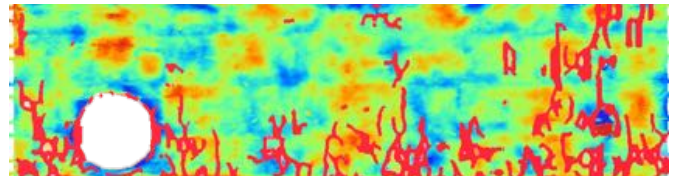
Fig.18:   Map of wearing, scaffolding, and cracks

5.   RESULTS AND EVALUATION

Scaffolding regions, wearing regions, and cracks are detected using our method. These deteriorations can be unified on the same difference map, as shown in Fig. 18.

We evaluated calculation time for detecting deterioration. Tab.1 shows the number of points. In this evaluation, a very large number of points were processed.

Tab. 2 shows CPU time for detecting wearing, scaffolding, and cracks. Since we used two different methods, we described CPU time for each method. CPU time was measured on a PC with 16 GB of RAM and Intel Core i5 - 4440 @ 3.10 GHz CPU.

The result shows that calculation time is practically sufficient. It took relatively long time to detect cracks, because cracks were detected from each of 12 point-clouds, and the results were integrated.

6.   CONCLUSION

In this paper, we proposed methods for detecting scaffolding, wearing and cracks on furnace walls. We detected deterioration as differences between the reference surface and measured points. We generated the reference surfaces using B-spline surfaces. We controlled the resolution of the reference surface using the number of control points. We used low-resolution reference surfaces for detecting wearing and scaffolding regions, and high-resolution reference surfaces for detecting cracks. For detecting cracks, we extracted cracks from each point-cloud and merged them. In our evaluation, the calculation time was practically sufficient even if a large number of points were processed.

In the future work, we would like to investigate methods to determine adequate resolutions for detecting various sizes of deteriorations. In addition, we would like to enhance our method to detect other types of deterioration on various facilities. We also would like to verify the reliability of our method by comparing with precise measurement.

REFERENCES

[1] Niwa, Takeru., and Masuda, Hiroshi. "Interactive collision Detection for engineering plants based on large-scale point-clouds." *Computer-Aided Design and Applications*, 13.4 (2016): pp. 511-518. https://doi.org/10.1080/16864360.2015.1131546

[2] Okamoto, Hiroki., and Masuda, Hiroshi. "A point-based virtual reality system for supporting product development" *ASME 2016 International Design Engineering Technical Conferences and Computers and Information in Engineering Conference. American Society of Mechanical Engineers* (2016) http://dx.doi.org/10.1115/DETC2016-59756

[3] Masuda, Hiroshi., and Ichiro Tanaka. "As-built 3D modeling of large facilities based on interactive feature editing." *Computer-Aided Design and Applications* 7.3 (2010): pp. 349-360. http://dx.doi.org/10.3722/cadaps.

[4] Masuda, Hiroshi., Niwa, Takeru. Tanaka, Ichiro., and Matsuoka, Ryo. "Reconstruction of polygonal faces from large-scale point-clouds of engineering plants." *Computer-Aided Design and*

Applications 12.5 (2015): pp.555-563. http://dx.doi.org/10.1080/16864360.2015.1014733

[5] Kawashima, Kazuaki., Kanai, Satoshi., and Date, Hiroaki. "As-built modeling of piping system from terrestrial laser-scanned point clouds using normal-based region growing." *Journal of Computational Design and Engineering* 1.1 (2014): pp. 13-26. http://dx.doi.org/10.7315/JCDE.2014.002

[6] Nan, Liangliang., Andrei, Sharf., Hao, Zhang., Daniel, Cohen-Or. and Baoquan, Chen. "Smartboxes for interactive urban reconstruction." *ACM Transactions on Graphics (TOG)* 29.4 (2010): pp. 93. http://dx.doi.org/10.1145/1778765.1778830

[7] Tang, Pingbo., Daniel, Huber., Burcu, Akinci., Alan M. Lytle. and Robert R. Lipman. "Automatic reconstruction of as-built building information models from laser-scanned point clouds: A review of related techniques." *Automation in construction* 19.7 (2010): pp. 829-843. http://dx.doi.org/10.1016/j.autcon.2010.06.007

[8] Mizoguchi, Tomohiro., Koda, Yasuhiro., Iwaki, Ichiro., Wakabayashi, Hiroyuki., Kobayashi, Yoshikazu., Shirai, Kenji., Hara, Yasuhiko., and Hwa-SooLee. "Quantitative scaling evaluation of concrete structures based on terrestrial laser scanning." *Automation in Construction* 35 (2013): pp. 263-274. http://dx.doi.org/10.1016/j.autcon.2013.05.022

[9] Nespeca R. and Livio De Luca. "Analysis, Thematic Maps and Data Mining from Point Cloud to Ontology for Software Development", *ISPRS-International Archives of the Photogrammetry, Remote Sensing and Spatial Information Sciences* (2016): pp. 347-354. http://dx.doi.org/10.5194/isprs-archives-XLI-B5-347-2016

[10] Shinozaki, Yuki., Kohira, Keisuke., and Masuda, Hiroshi. "Detection of deterioration of furnace walls using large-scale point-clouds." *Computer-Aided Design and Applications* (2018): pp. 1-10. https://doi.org/10.1080/16864360.2017.1419645

[11] FARO Laser Scanner Focus 3D X130, http://www.faro.com, 2014.

[12] Lukács, Gabor., Ralph, Martin., and Dave, Marshall. "Faithful least-squares fitting of spheres, cylinders, cones and tori for reliable segmentation." *European conference on computer vision*. Springer, Berlin, Heidelberg, (1998): pp. 671-686. https://doi.org/10.1007/BFb0055697

[13] Masuda, Hiroshi., and Tanaka, Ichiro. "Extraction of surface primitives from noisy large-scale point-clouds." *Computer-Aided Design and Applications* 6.3 (2009): pp. 387-398. http://dx.doi.org/10.3722/cadaps. 2009.387-398

[14] Schnabel, Ruwen., Roland, Wahl. and Reinhard, Klein. "Efficient RANSAC for point-cloud shape detection." *Computer graphics forum*. Vol. 26. No. 2. Blackwell Publishing Ltd, (2007): pp. 214-226. http://dx.doi.org/10.1111/j.1467-8659.2007.01016.x

[15] Weiss, Volker., V.Andor., L.Renner,G., and Várady, T.. "Advanced surface fitting techniques." *Computer Aided Geometric Design* 19.1 (2002): pp. 19-42. https://doi.org/10.1016/S0167-8396(01)00086-3